Available online at www.sciencedirect.com
ScienceDirect
Journal of the European Ceramic Society 31 (2011) 1733–1739
www.elsevier.com/locate/jeurceramsoc

Examination of the co-sintering process of thin 8YSZ films obtained by dip-coating on in-house produced NiO–YSZ

Hanna Tikkanen [a,b,*], Crina Suciu [b], Ivar Wærnhus [b], Alex C. Hoffmann [a,b]

[a] University of Bergen, Institution of Physics and Technology, Allégaten 55, NO-5007 Bergen, Norway
[b] Prototech AS, Fantoftveien 38, NO-5075 Bergen, Norway

Received 9 December 2010; received in revised form 2 March 2011; accepted 7 March 2011
Available online 31 March 2011

Abstract

Preparation conditions for obtaining dense 8YSZ electrolyte films by dip-coating on NiO–YSZ anode electrode substrates for SOFC application were investigated with focus on the co-sintering process. The NiO–YSZ substrates were prepared from nanoparticles which were obtained by a single modified sol–gel process using sucrose and pectin as organic precursors. The microstructure and the morphology of the product powders were analyzed by X-ray diffraction and TEM. A thin film of 8YSZ was obtained by a single-step dip-coating process using phosphate ester (PE) as dispersant and polyvinyl butyral (PVB) as binder. The microstructure of the sintered films was analyzed with SEM. The effect of the sinterability of the anode substrate on the 8YSZ film quality was studied. Fully dense electrolyte films were obtained on anode substrates which held a linear shrinkage of ∼23%. The use of substrates with a linear shrinkage below 23%, resulted in a poorly densified 8YSZ microstructure.

Keywords: Sol–gel processes; Dip-coating; Films; Microstructure; Fuel cells

1. Introduction

A solid oxide fuel cell (SOFC) is a device that converts the chemical energy of fuels directly into electricity by electrochemical oxidation.[1] The process is not restricted by Carnot efficiency limits and high thermodynamic efficiency can be obtained. Other advantages are that SOFCs can operate on many different fuels and emit negligible NO_x and SO_x pollution.

In recent years, many active investigations have been made in SOFCs. However, wide commercialization of fuel cell technology has so far not taken place. The operating temperature (800–1000 °C) of current SOFCs sets stringent requirements on the materials used in the stack as well as affecting the durability and life-time of the system.[1] Reducing the operating temperatures below 800 ° C would mean that a wider range of materials could be used thus reducing the costs of the total system. The current focus in research in SOFCs is material development and reduced-temperature operation.

A SOFC produces electricity through the reduction of oxygen to O^{2-} ions at the cathode, transportation of these ions through the electrolyte to electrolyte/anode interface and by oxidation of the fuel with O^{2-} ions at the anode.[1] A standard material used for the electrolyte is yttria (Y_2O_3) stabilized zirconia (ZrO_2), YSZ, which is an oxide ion conductor at temperatures from 600 to 1000 °C. However, reducing the operating temperature below 800 ° C increases drastically the electrolyte resistivity and decreases the ionic conductivity. To overcome the ohmic drop through the electrolyte at reduced-temperature new types of solid electrolytes with higher oxide ion conductivity, such as doped ceria and lanthanum gallate, are being studied.[1] An alternative approach to decrease the resistivity of the electrolyte, is to reduce the thickness of the electrolyte. This can be done by electrode-supported cells where a thin film of YSZ is deposited on an electrode support. For this purpose, anode-supported cells are favoured over cathode-supported cells because the co-sintering of the cathode material and YSZ is more problematic.[1–4]

There are different methods to obtain thin films, including physical vapor deposition (PVD) such as sputtering[5] and pulsed laser deposition,[6] chemical vapor deposition (CVD),[7] plasma technologies[8] and electrophoretic deposition (EPD).[2–4,9–11] However, for PVD and CVP methods sophisticated and expen-

* Corresponding author at: Prototech AS, Fantoftveien 38, NO-5075 Bergen, Norway. Tel.: +47 94 14 03 46; fax: +47 56 57 41 14.
E-mail addresses: hanna.tikkanen@prototech.no, Hanna-Mari.Tikkanen@ift.uib.no (H. Tikkanen).

0955-2219/$ – see front matter © 2011 Elsevier Ltd. All rights reserved.
doi:10.1016/j.jeurceramsoc.2011.03.015

sive equipment is required. EPD is a cost-effective colloidal method with the pre-requisite for the deposition substrate to be conductive or to be coated with a conductive layer.[2–4,9–12] Dip-coating is a wet-chemical process that has been used widely in order to obtain thin films.[13–24] It is a low-cost method that can be scaled for industrial purposes. The substrates used for dip-coating can have planar, cylindrical or complex geometries.

Dip-coating process is similar to slip-casting.[13] When a porous substrate is brought in contact with YSZ suspension, capillary action due to the pores in the substrate withdraws the liquid from the suspension. As the liquid filters into the substrate a YSZ cast is formed at the boundary of the substrate and the suspension.

Careful adjustment of the chemistry of the suspension by using additives, gives a stable suspension with high solid concentration and low viscosity. The issues involved in generating a suspension with suitable properties are almost the same for various deposition techniques, such as electrophoretic deposition, dip-coating and tape-casting. Results in recent studies by Zhitomirsky and Petric indicate that ethanol-phosphate ester (PE)–polyvinyl butyral (PVB) system is an effective medium for electrophoretic deposition (EPD) of ceramic materials for solid oxide fuel cell application.[9,10] PE is a dispersant material which functions as an effective electrostatic stabilizer. In addition, it acts as a steric dispersant by physically prohibiting particles to coming into contact with each other. PVB is a widely used polymer and an important binder in ceramic processes such as tape casting[25] and dip-coating.[20,23] It provides the backbone for the green body by giving strength and flexibility that holds the entire chemical system together for further processing.[25] In addition, studies have been made which indicate that PVB can also serve as an effective dispersant.[26–28] The PVB molecule has alcohol functional groups as well as butyral segments. The butyral segments serve as a steric stabilizer upon polymer adsorption on the ceramic particle surface.[10] The adsorption takes place by hydrogen-bond formation with the hydroxyl groups on particle surface.[27] The bath composition presented by Zhitomirsky and Petric was applied to obtain thin 8YSZ films by dip-coating method in this work.

Nanomaterials as precursors for SOFC compounds have been of great interest. It has been shown that by using NiO–YSZ nano-composite powder the performance and durability of single SOFC cells are improved due to homogeneous structure and larger thriple-phase boundaries, TPBs.[15–17,19,24] In this work, NiO–YSZ nanoparticles were obtained via a modified sol–gel method using sucrose and pectin as organic precursors. It has been demonstrated in earlier work that nanoparticles suitable for the SOFC application can be manufactured with this method.[29–31] The obtained nanopowder was then pressed into pellets and used as substrates for dip-coating of 8YSZ.

For a fuel cell to work, the electrolyte has to be dense and the electrodes have to be porous. As the electrolyte film is sintered together (co-sintered) with the deposition substrate, the sintering conditions are important.

Densification of ceramic coatings is typically accompanied by dimensional changes upon sintering. As coatings suffer linear shrinkage, one critical issue is how to avoid cracking.[32] Other defects occuring might be voids and pores. Multiple dip-coating and sintering steps have been used in the literature to eliminate the cracks and defects, which have been formed during either drying or sintering.[13,14,21–23] However, the green film thickness also increases with the dip-coating time increasing.[14,15,21] One approach to minimize flaws is to use a substrate that also shrinks during sintering. Pre-sintered or un-sintered electrode substrates have been used in SOFC applications.[32] It is reported in the literature that the densification of the 8YSZ film is affected by the sinterability of the anode-support.[12,22] Substrate shrinkage of above 15% has been found to produce fully densified GDC electrolyte films under single dipping conditions.[20] Anode tubular support shrinkage of ∼20% was sufficient to produce fully densified YSZ layers.[22] In addition to large shrinkage, the anode substrate should have enough mechanical strength after pre-sintering so that it is easy to handle during the deposition process.[11]

The discussion in the previous paragraph shows the properties of the substrate, which is the anode support, to be crucial for the success of the co-sintering process forming the electrolyte film and the finished anode together. The properties of the substrate are to a large extent determined in the pre-sintering process. For these reasons, the effect of the pre-sintering temperature of the anode support on the quality of the obtained 8YSZ film was studied.

2. Experiments

The NiO–YSZ nanoparticles were obtained by a modified sol–gel method. Zirconium tetracloride ($ZrCl_4$, 99.5+%, Aldrich), yttrium nitrate ($Y(NO_3)_3{\cdot}6H_2O$, 99.9%, Aldrich) and nickel nitrate heksahydrate ($Ni(NO_3)_2{\cdot}6H_2O$, Sigma–Aldrich) were used as starting material. The approriate quantities to obtain 8 mol% of yttria-stabilized zirconia was calculated and used. The appropriate quantities to obtain a final powder composition NiO–YSZ of ratio 50:50 was calculated and used. The amounts of the starting compounds are presented in Table 1. The weighted starting compounds were dissolved in deionized water under magnetic stirring. The clear solutions were then transferred in alumina dishes and set on a sand bath. Sucrose and pectin were added to the solutions in a ratio of 50:5, respectively. The solutions were allowed to dry under stirring and a dry gel was formed. The final dry gel was then calcinated at a temperature of 1000 ° C to form the NiO–YSZ nanoparticles. The calcination program applied had a heating plateau at 500 ° C for 1 h to burn of the organic material in the gel. A schematic presentation of obtaining the nanopowder is presented in Fig. 1.

The obtained NiO–YSZ nanoparticles were investigated using TEM and XRD.

The obtained NiO–YSZ nanopowders were milled with zirconia balls in deionized water for 24 h and set to dry. The dried powder was then mortered, sieved and pressed to pellets (d = 20 mm) by a uniaxial press (1200 psi = 8.3 MPa). The pressed substrates were presintered for 2 h at various temperatures (1000, 1100, 1200 and 1300 °C) with a heating rate of 200 °C/h.

Table 1
The starting compounds.

$Ni(NO_3)_2{\cdot}6H_2O$ (g)	$ZrCl_4$ (g)	$Y(NO_3)_3{\cdot}6H_2O$ (g)	Sugar (g)	Pectin (g)	H_2O (ml)
27.25	10.20	2.92	50	5	400

The suspension for dip-coating was prepared by mixing 10 g of 8YSZ (TZ-8Y, Tosoh) and 0.15 g of PE and 0.30 g of PVB with 100 ml ethanol (technical ethanol, KEMETYL). The suspensions were then ultrasonically mixed for 1 h in an ultrasonic bath. The porous NiO–YSZ substrate was attached to a stainless steel wire. The electrolyte films were obtained by dip-coating the porous substrate in the suspension for 30 s. The green films were dried at room temperature and sintered at 1400 ° C for 2 h. The sintering program applied had a heating plateau at 600 ° C for 1 h to burn of the organic material in the green 8YSZ film. The morphology of the sintered 8YSZ thin films was studied by scanning electron microscopy (SEM, Zeiss Supra 55VP).

The linear shrinkage of the green 8YSZ body and the NiO–YSZ substrates pre-sintered at different temperatures were studied by a dilatometer (Linseis, L75V). The anode samples for the dilatometer were pressed pellets ($p = 1200$ psi) which were cut to smaller pieces and then pre-sintered at different temperatures (1000, 1100, 1200 and 1300 °C) with a heating rate of 200 °C/h. The 8YSZ green bodies were prepared by allowing the suspensions used for dip-coating to settle and removing the precipitated powder. The precipitated powder was then formed in a cylinder shape. The linear shrinkage of the samples was measured using the same sintering program as in the co-sintering step.

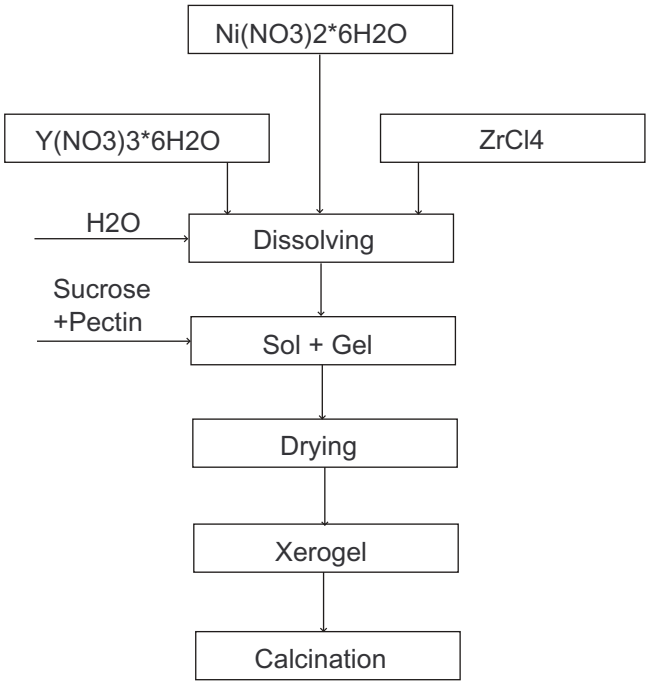

Fig. 1. A schematic presentation of obtaining the NiO–YSZ nanopowder.

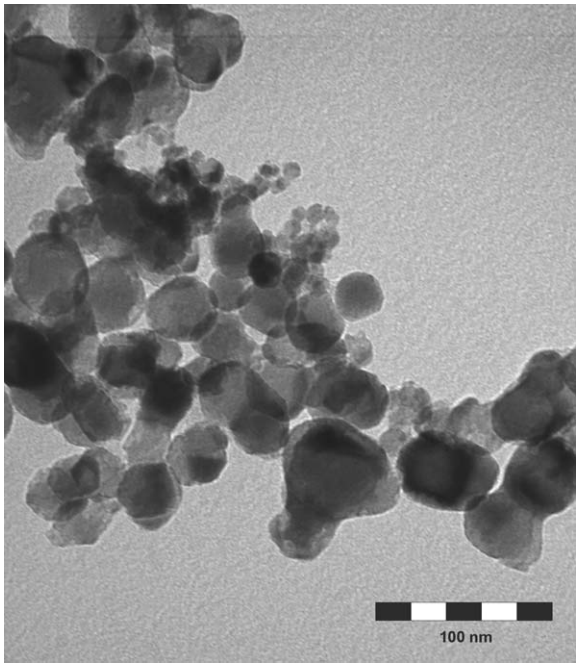

Fig. 2. A TEM image of the NiO–YSZ powder calcinated at 1000 ° C for 2 h.

3. Results and discussion

3.1. Nanopowder

A TEM (transmission electron microscopy) image of the obtained calcinated NiO–YSZ nanoparticles is presented in Fig. 2. The particle size was calculated by measuring 10 particles from the image. The particle size varied from 30 to 60 nm with the majority of the particles being just over 30 nm. Unfortunately, the two types of particles (NiO and YSZ) cannot be distinguished visibly.

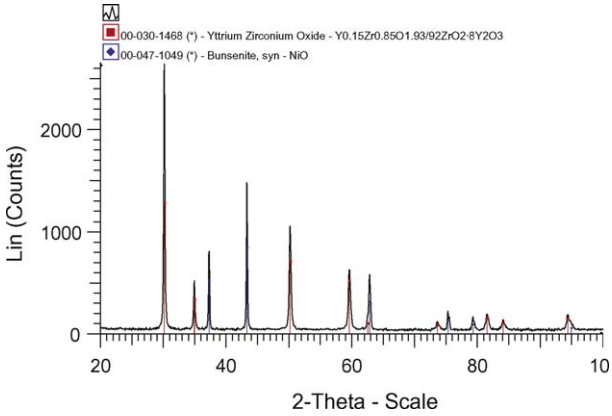

Fig. 3. XRD pattern of the NiO–YSZ powder calcinated at 1000 ° C for 2 h.

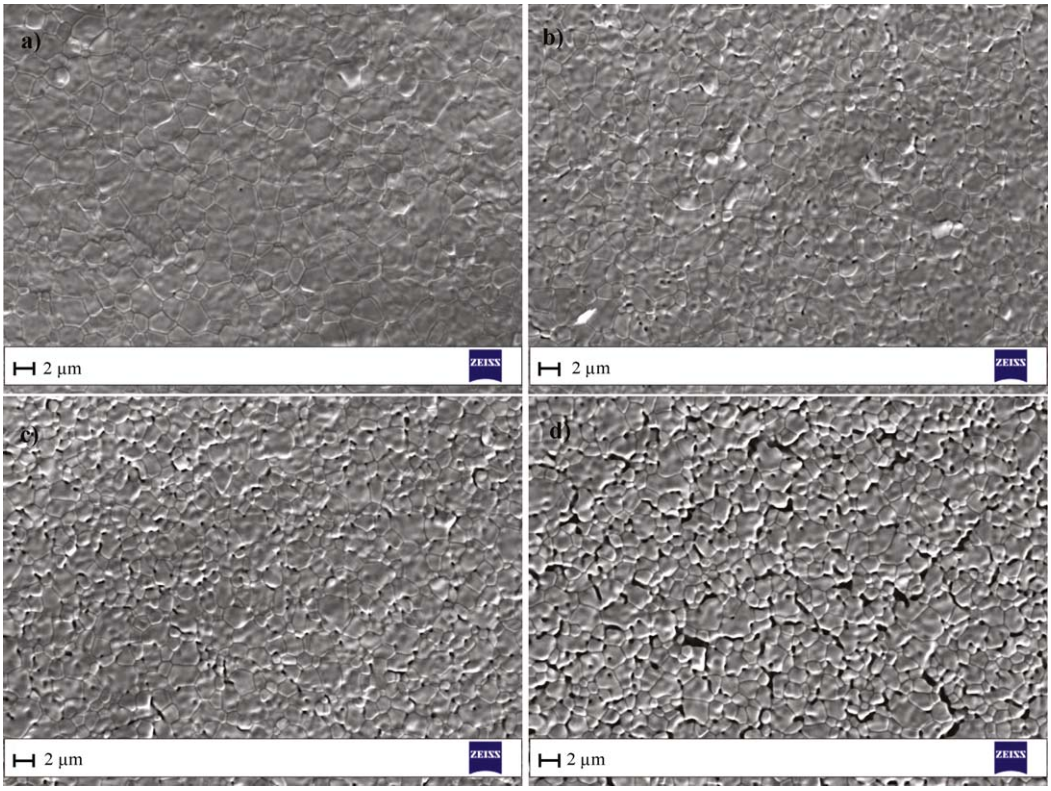

Fig. 4. A SEM image of a sintered 8YSZ film on anode substrate pre-sintered at (a) 1000 °C, (b) 1100 °C, (c) 1200 ° C and (d) 1300 ° C for 2 h.

In Fig. 3 the X-ray spectrum of the NiO–YSZ powder calcinated at 1000 ° C is presented. The X-ray diffraction measurements were carried out with Cu K-α radiation on a Bruker diffractometer from 20 ° to 100 ° with a step size of 0.02 ° and a counting rate of 3 s per scanning step. The spectrum shows the presence of two phases: NiO and YSZ, both in the $Fm-3m$ cubic type structure. There is no indication of other phases present. The mean crystallite size can be calculated from the full widht at half maximum (FWHM) from the obtained diffraction pattern. For particles calcinated at 1000 ° C the crystallite size for NiO and YSZ was calculated to be 53 nm and 31 nm, respectively. The TEM investigations were in good agreement with the XRD data.

3.2. Film deposition and film quality

The dispersion of the 8YSZ particles is an important factor determining the compact density. Fully dispersed systems lead to high-density compacts and subsequently dense and homogeneous electrolyte films after sintering.[14] Zhitomirsky and Petric observed that PE is an effective dispersing agent for 8YSZ in ethanol and isopropanol suspensions.[9,10] Addition of PE stabilized the suspension from settling and a remarkable increase in the deposition weight was observed when the concentration of PE was increased to the range up to 1 g/l.[10] After this the increase in deposition weight was less significant. Sedimentation experiments showed that addition of PE up to 2–3.5 g/l resulted in increasing stability of YSZ.[9] However, pinholes were observed in the deposits when PE concentration was higher than $\sim 2--2.5$ g/l.[10] The amount of 1.5 g/l PE was used in this study to ensure full dispersion.

The use of additives containing phosphorus in the preparation process of the electrolyte film might raise some issues regarding the sintering process and the SOFC performance. In a study by Gao and Guo, doping of barium zirconate with P_2O_5 affected the sintering behaviour of the ceramic.[33] The microstructure became denser by the addition of P_2O_5. Residues of P_2O_5 were also found to produce reaction products with the ceramic indicating that a liquid-phase sintering mechanism was present. Regarding the actual operation of an SOFC, phosphorus has been reported to interact strongly with nickel leading to a irreversible cell degradation.[34,35] In addition, introducing phosphorus in the fuel has been found to result in the formation of zirconium phosphate in the anode affecting thus its oxide ion conductivity.[35]

Zhitomirsky and Petric discussed the problems of using PE as a dispersing agent for the EPD method.[10] The fact that PE has been found to leave traces of phosphorus in ceramic bodies obtained by tape casting was noted. The concentration of PE needed to stabilize suspension for tape casting was stated to be low, though. As Zhitomirsky and Petric pointed out in their discussion, the PE particle concentrations are much lower in deposits obtained by EPD than in ceramics prepared by tape casting. In contrast to the tape casting process, where all the PE in the suspension is taken up in the ceramic body, in EPD only the PE molecules adsorbed onto the particles are incorporated in the final film. Hence, the risk of PE intercalation was considered to be lower in deposits obtained by EPD. Since also in dip-coating only the adsorbed PE molecules are present in deposits,

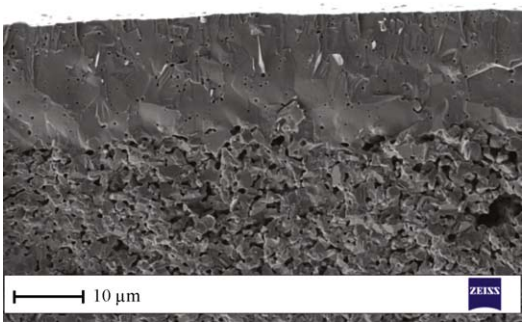

Fig. 5. A SEM image of a sintered 8YSZ film on an anode substrate pre-sintered at 1000 ° C for 2 h.

the present authors suggest that the arguments given above are valid also here.

Drying of the green film is a critical process. When a wet body undergoes drying, tensile stress is developed in the coating.[32,36] The typical problem that one faces when drying a ceramic coating is cracking of the film. Organic binders can be used to hold together the ceramic green body when dried. To avoid cracking Zhitomirsky and Petric added PVB to the suspension.[9,10] Addition of PVB binder up to 2.5–3 g/l resulted in better adhesion of the deposits.[9] The bath composition was later optimized and deposits obtained from 8YSZ suspensions containing 1–1.5 g/l of PE and 1–2 g/l of PVB were dense and crack-free.[10] In this work 3.0 g/l of PVB was used.

Deposition was obtained on all the NiO–YSZ substrates. However, the wetting properties of the anode substrate surface to the 8YSZ suspension became visibly lower when the anode substrates were pre-sintered at 1300 °C. This was due to the reduced porosity of the anode.[20] Crack-free green films were obtained after drying for 24 h.

The pre-sintering temperature of the substrate was found to be important for the quality of the final electrolyte film. Densification of the 8YSZ films decreased with increasing pre-sintering temperature of the NiO–YSZ substrate. Fig. 4 presents sintered 8YSZ films on NiO–YSZ substrates pre-sintered at (a) 1000 °C, (b) 1100 °C, (c) 1200 ° C and at (d) 1300 °C, respectively. It is evident that the film on the substrate pre-sintered at a higher temperature exhibit more pores and voids. In addition, the 8YSZ film on anode substrate pre-sintered at 1300 ° C exhibited severe cracking.

Fig. 5 presents the cross-section of an 8YSZ film on a porous substrate pre-sintered at 1000 °C. The 8YSZ electrolyte is dense with limited and isolated closed pores and adheres well to the anode substrate. The thickness of the 8YSZ electrolyte is about 15 µm. The films appear to be crack-free.

The anode substrate should be sufficiently porous for the gas transport to take place during cell operation. The anode substrate in Fig. 5 shows a relatively dense microstructure. In this study, the anode was prepared without the addition of pore formers. However, it is expected that the reduction of NiO to Ni will increase the porosity.[13,21] But since too low an anode porosity might be problematic for the reduction to happen in the first place, the effect of the addition of pore formers during anode preparation on the dip-coating process will be studied in future work.

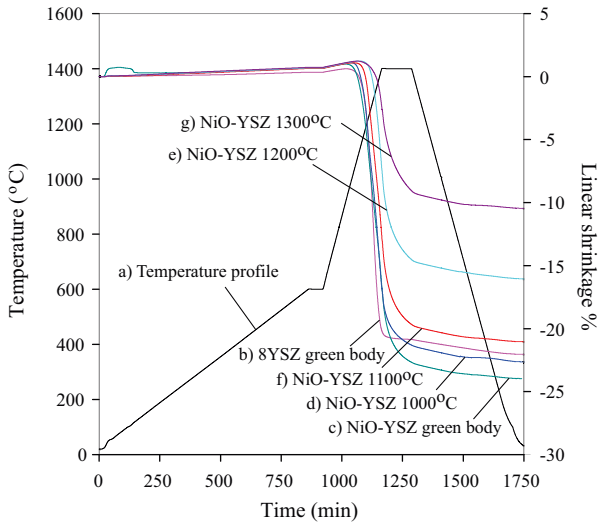

Fig. 6. (a) Temperature profile and the shrinkage behaviour of (b) 8YSZ green body, (c) NiO–YSZ green body, (d) NiO–YSZ pre-sintered at 1000 °C, (e) NiO–YSZ pre-sintered at 1100 °C, (f) NiO–YSZ pre-sintered at 1200 ° C and (g) NiO–YSZ pre-sintered at 1300 °C.

3.3. Sintering behaviour

The sintering behaviour of the 8YSZ electrolyte and the NiO–YSZ anode material was quantified by dilatometric measurements. The materials tested in the dilatometer were produced so as to match the SOFC components as closely as possible. For the anode materials, actual substrates were divided into strips for testing. For the electrolyte materials, suspensions of the YSZ powder, matching the suspensions used in the dip-coating process, were allowed to settle and the beds formed were then dried in the same way as the dip-coating films to produce the green bodies for testing in the dilatometer. Fig. 6 shows the linear shrinkage that the following samples undergo during the co-sintering process: 8YSZ green body, anode green body and anode bodies pre-sintered at 1000, 1100, 1200 and 1300 °C. The densification of the 8YSZ starts at about 1000 ° C and that of the anode green body at about 900 °C.

Table 2 summarizes the relative shrinkage of the anode substrates as a function of pre-sintering temperature. These results indicate that the linear shrinkage of the substrates during the final co-sintering process increased with decreasing pre-sintering temperature. The linear shrinkage of the anode green body reached a value of ∼24% at 1400 ° C and that of the anode samples pre-sintered at 1000, 1100, 1200 and 1300 ° C reached a value of ∼23, 21, 16 and 10% at 1400 °C, respectively. These

Table 2
The relative shrinkage of the anode substrates as a function of pre-sintering temperature

Pre-sintering temperature (°C)	0	1000	1100	1200	1300
Relative shrinkage (%)	24	23	21	16	10

results, together with the previously shown results for the quality of the electrolyte films, show that the densification of the substrate during the co-sintering step should be comparable to that of the electrolyte film to obtain films with an acceptable quality. An overall anode support shrinkage of 23% was needed to ensure the full densification of the 8YSZ film.

There is probably no universal threshold for sufficient substrate densification. The dip-coating process normally leads to the formation of a hexagonal closed-packed arrangement of the particles in the deposited film.[37] Assuming isotropic shrinkage and an original volume of $V = abc$, the volume after a fractional linear shrinkage of x is: $V_s = abc(1-x)^3$. The voidage fraction, ϵ, of the original material is then:

$$\epsilon = \frac{V - V_s}{V} = 1 - (1-x)^3 \quad (1)$$

The voidage of a material consisting of uniformly sized spheres in a hexagonal-close-packed (hcp) arrangement is about $1 - 0.740 = 0.260$, and such a material will, according to Eq. (1), undergo a linear fractional shrinkage of $x = 1 - (1-\epsilon)^{1/3} = 0.0955$ or about 10% for full densification (see also[20]). In our case the linear shrinkage was much higher than this, namely about 23%, which, according to Eq. (1), corresponds to a voidage fraction in the original green body of 0.543. Such a value is reasonable, however, since the material was not subjected to any pressure in forming the green body. It is known[38] that the absolute size of "dry" particles influences the void fraction of the beds they form if the particles are very small, the interparticle forces preventing densification of the beds beyond a certain point. Although the interparticle forces in liquids are likely to be less, the present particles are very small so that interparticle forces may well prevent densification of the green body to the hcp voidage.

Obtaining high quality electrolyte films on anode-supported fuel cells is a function of many factors. This study focused on the the co-sintering process. The results show that the pre-sintering temperature, which subsequently determines the further sinterability of the substrate at the co-sintering stage, is one important factor in fabricating dense electrolyte films for SOFC applications. Further work include to optimize the dip-coating process and performing cell testing measurements.

4. Conclusions

In this work, dip-coating was used to obtain 8YSZ films on porous NiO–YSZ substrates. This technique was used because it is a simple and cost-effective method for fabrication of thin films on planar substrates.

The substrates were prepared of in-house produced nanopowder by a single sol–gel method using sucrose and pectin as precursors. Crack-free 8YSZ green films were obtained after drying using PE and PVB as dispersant and binder, respectively.

Densification of the electrolyte layer on the anode substrates is important for anode-supported cells. The densification of the 8YSZ films was affected by the pre-sintering temperature of the anode support. The quality of the 8YSZ electrolyte film increased with decreasing pre-sintering temperature of the NiO–YSZ substrate. By tuning the linear shrinkage of the deposition substrate to match the shrinkage of the 8YSZ film during sintering, dense deposits can be obtained.

The results indicate that the in-house produced nanopowder can be used as an electrode support in an anode-supported cell. In addition, the results indicate that dip-coating is an effective method for obtaining thin electrolyte films for SOFC applications.

Acknowledgements

The authors wish to acknowledge the NFR (Norwegian Research Council) for funding this project. Also, the authors are grateful to Senior Engineer Egil Erichsen (The Electron Microscopy Laboratory, University of Bergen) for help using the TEM and SEM. In addition, the authors wish to acknowledge PhD Eugen Dorolti (Babes-Bolyai University, Physics Faculty, Romania) for performing the XRD measurements on the anode powder.

References

1. Singhal SC, Kendall K. *High temperature solid oxide fuel cells: fundamentals, design and applications*. 1st ed Elsevier Ltd; 2003.
2. Ishihara T, Shimose K, Kudo T, Nishiguchi H, Akbay T, Takita Y. Preparation of yttria-stabilized zirconia thin films on strontium-doped $LaMnO_3$ cathode substrates via electrophoretic deposition for solid oxide fuel cells. *Journal of the American Ceramic Society* 2000;**83**:1921–7.
3. Yang K, Shen JH, Yang KY, Hung IM, Fung KZ, Wang MC. Characterization of the yttria-stabilized zirconia thin film electrophoretic deposited on $La_{0.8}Sr_{0.2}MnO_3$ substrate. *Journal of Alloys and Compounds* 2007;**436**:351–7.
4. Lee YH, Kuo CW, Shih CJ, Hung IM, Fung KZ, Wen SB, et al. Characterization on the electrophoretic deposition of the 8 mol% yttria-stabilized zirconia nanocrystallites prepared by sol–gel process. *Materials Science and Engineering A* 2007;**445–446**:347–54.
5. Rey-Mermet S, Yan Y, Sandu C, Deng G, Muralt P. Nanoporous YSZ film in electrolyte membrane of micro-solid oxide fuel cell. *Thin Solid Films* 2010;**518**:4743–6.
6. Garbayo I, Tarancon A, Santiso J, Peiro F, Alarcon-LLado E, Cavallaro A, et al. Electrical characterization of thermomechanically stable YSZ membranes for micro solid oxide fuel cells applications. *Solid State Ionics* 2010;**181**:322–31.
7. Gelfond NV, Bobrenok OF, Predtechensky MR, Morozova NB, Zherikova KV, Igumenov IK. Chemical vapor deposition of electrolyte thin films based on yttria-stabilized zirconia. *Inorganic Materials* 2009;**45**:659–65.
8. Mirahmadi A, Pourmalek M. Improvement of plasma-sprayed YSZ electrolytes for solid oxide fuel cells by alumina addition. *Ionics* 2010;**16**:447–53.
9. Zhitomirsky I, Petric A. Electrophoretic deposition of ceramic materials for fuel cell application. *Journal of the European Ceramic Society* 2000;**20**:2055–61.
10. Zhitomirsky I, Petric A. Electrophoretic deposition of electrolyte materials for solid oxide fuel cells. *Journal of Material Science* 2004;**39**:825–31.
11. Will J, Hruschka MKM, Gubler L, Gauckler LJ. Electrophoretic deposition of zirconia on porous anodic substrates. *Journal of American Ceramic Society* 2001;**84**:328–32.
12. Hosomi T, Matsuda M, Miyake M. Electrophoretic deposition for fabrication of YSZ electrolyte film on non-conducting porous NiO–YSZ composite substrate for intermediate temperature SOFC. *Journal of the European Ceramic Society* 2007;**27**:173–8.
13. Xia C, Zha S, Yang W, Peng R, Peng D, Meng G. Prepararion of yttria stabilized zirconia membranes on porous substrates by a dip-coating process. *Solid State Ionics* 2000;**133**:287–94.

14. Zhang Y, Gao J, Peng D, Guangyao M, Liu X. Dip-coating thin yttria-stabilized zirconia films for solid oxide fuel cell application. *Ceramics International* 2004;**30**:1049–63.
15. Kim SD, Hyun SH, Moon J, Kim JH, Song RH. Fabrication and characterization of anode-supported electrolyte thin films for intermediate temperature solid oxide fuel cells. *Journal of Power Sources* 2005;**139**:67–72.
16. Kim SD, Moon H, Hyun SH, Moon J, Kim J, Lee HW. Performance and durability of Ni-coated YSZ anodes for intermediate temperature solid oxide fuel cells. *Solid State Ionics* 2006;**177**:931–8.
17. Kim SD, Moon H, Hyun SH, Moon J, Kim J, Lee HW. Nano-composite materials for high-performance and durability of solid oxide fuel cells. *Journal of Power Sources* 2006;**163**:392–7.
18. Gaudon M, Laberty-Robert C, Ansart F, Stevens P. Thick YSZ films prepared via a modified sol–gel route: Thickness control (8–80 μm). *Journal of the European Ceramic Society* 2006;**26**:3153–60.
19. Kim SD, Lee JJ, Moon H, Hyun SH, Moon J, Kim J, et al. Effects of anode and electrolyte microstructures on performance of solid oxide fuel cells. *Journal of Power Sources* 2007;**169**:265–70.
20. Yamaguchi T, Suzuki T, Shimizu S, Fujishiro Y, Awano M. Examination of wet coating and co-sintering technologies for micro-SOFCs fabrication. *Journal of Membrane Science* 2007;**300**:45–50.
21. Liu RZ, Wang SR, Huang B, Zhao CH, Li JL, Wang ZR, et al. Dip-coating and co-sintering technologies for fabricating tubular solid oxide fuel cells. *Journal of Solid State Electrochemistry* 2009;**13**:1905–11.
22. Zhang L, He HQ, Kwek WR, Ma J, Tang EH, Jiang SP. Fabrication and characterization of anode-supported tubular solid-oxide fuel cells by slip casting and dip coating techniques. *Journal of the American Ceramic Society* 2009;**92**:302–10.
23. Wang Z, Sun K, Shen S, Zhou X, Qiao J, Zhang N. Effect of co-sintering temperature on the performance of SOFC with YSZ electrolyte thin films fabricated by dip-coating method. *Journal of Solid State Electrochemistry* 2010;**14**:637–42.
24. Lee JJ, Moon H, Park HG, Yoon DI, Hyun SH. Applications of nano-composite materails for improving the performance of anode-supported electrolytes of SOFCs. *International Journal of Hydrogen Energy* 2010;**35**:738–44.
25. Mistler RE, Twiname ER. *Tape casting-theory and practice*. 1st ed. Ohio, US: The American Ceramic Society; 2000.
26. Bhattacharjee S, Paria MK, Maiti HS. Polyvinyl butyral as a dispersant for barium titanate in non-aqueous suspension. *Journal of Materials Science* 1993;**28**:6490–5.
27. Jean JH, Yeh SH, Chen CJ. Adsorption of polyvinyl butyral in non-aqueous ferrite suspension. *Journal of Materials Research* 1997;**12**:1062.
28. Mukherjee A, Khan R, Bera B, Maiti HS. I: Dispersability of robust alumina particles in non-aqueous solution. *Ceramics International* 2008;**34**: 523–9.
29. Suciu C, Hoffmann AC, Dorolti E, Tetean R. Ni/YSZ nanoparticles obtained by new sol–gel route. *Chemical Engineering Journal* 2008;**140**:586–92.
30. Suciu C, Hoffmann AC, Vik A, Goga F. Effect on process parameters on YSZ nanoparticles obtained by modified sol–gel route. *Chemical Engineering Journal* 2008;**138**:608–15.
31. Suciu C, Hoffmann AC, Kosinski P. Obtaining YSZ nanoparticles by sol–gel method with sucrose and pectin. *Journal of Materials Processing Technology* 2008;**202**:316–20.
32. Sarkar P, De D, Rho H. Synthesis and microstructural manipulation of ceramics by electrophoretic deposition. *Journal of Materials Science* 2004;**39**:819–23.
33. Gao DY, Guo RS. Densification and properties of barium zirconate ceramics by addition of P_2O_5. *Materials Letters* 2010;**65**:573–5.
34. Marina OA, Coyle CA, Thomsen EC, Edwards DJ, Coffey GW, Pederson LR. Degradation mechanisms of SOFC anodes in coal gas containing phosphorus. *Solid State Ionics* 2010;**181**:430–40.
35. Zhi MJ, Chen XQ, Finklea H, Celik I, Wu NQQ. Electrochemical and structural analysis of nickel-yttria-stabilized zirconia electrode operated in phosphorus-containing syngas. *Journal of Power Sources* 2008;**183**:485–90.
36. Ring TA. *Fundamentals of ceramic powder processing and synthesis*. 1st ed. Academic Press; 1996.
37. Wang Y, Zhou W. A review on inorganic nanostructure self-assembly. *Journal of Nanoscience and Nanotechnology* 2010;**10**:1563–83.
38. Hoffmann AC, Finkers HJ. A relation for the void fraction of randomly packed particle beds. *Powder Technology* 1995;**82**:197–203.